ORIGINAL ARTICLE

TMS Neuro-Cardiovascular Coupling in Vascular Compression Cranial Neuropathy

Adam Kirton, Carolyn Gunraj, Robert Chen

ABSTRACT: ***Background:*** Neurovascular compression (NVC) may cause cranial mononeuropathy but lacks a definitive diagnostic investigation. We hypothesized that the arterial pressure wave (APW) would interact at the neurovascular interface in NVC to inhibit transmission of transcranial magnetic stimulation (TMS) stimuli to affected muscles. ***Methods:*** We report a novel neurophysiological method coupling cardiovascular physiology with TMS. The electrocardiogram (ECG) and arterial pressure wave (APW) were coupled to triggering of cortical TMS in a patient with NVC-induced spinal accessory (CNXI) mononeuropathy. Outcome measures included motor evoked potential (MEP) amplitudes and firing probabilities of normal and affected trapezieus (TPZ). Values at intervals in proximity to the APW (40/80/120/160ms) were compared to baseline (800ms) using ANOVA and student t-test. ***Results:*** Electrocardiogram triggered TMS of CNXI pathways with 100% reliability. MEP amplitudes were decreased in proximity to the APW, particularly at 120ms (0.21±0.04 mV versus 0.39±0.10mV, p=0.003). TPZ firing probabilities were similarly inhibited (43.8% versus 88.2%, p=0.009). No effect of APW proximity was observed on the unaffected side (p=0.868). Procedures were well tolerated. ***Conclusions:*** Vascular compression causes CNXI mononeuropathy. Transcranial magnetic stimulation-cardiovascular coupling may evaluate neurovascular junction interactions and non-invasively diagnose NVC.

RÉSUMÉ: Couplage neuro-cardiovasculaire par SMT dans la neuropathie crânienne due à une compression vasculaire. ***Contexte :*** Une compression neuro-vasculaire (CNV) peut causer une mononeuropathie crânienne, mais les moyens d'en établir le diagnostic sont mal définis. Nous avons émis l'hypothèse que l'onde de pression artérielle (OPA) interagit au niveau de l'interface neuro-vasculaire dans la CNV pour inhiber la transmission de stimuli aux muscles atteints lors de la stimulation magnétique transcrânienne (SMT). ***Méthodes :*** Nous rapportons une nouvelle méthode neurophysiologique de couplage de la physiologie cardiovasculaire avec la SMT. L'électrocardiogramme (ECG) et l'onde de pression artérielle (OPA) ont été couplés à l'activation de la SMT chez un patient atteint de mononeuropathie du nerf spinal (NCXI) provoquée par une CNV. Nous avons mesuré les amplitudes et les probabilités de décharge des potentiels évoqués moteurs du muscle trapèze normal et du muscle trapèze atteint. Les valeurs enregistrées à intervalles à proximité de l'OPA (40/80/120/160 ms) ont été comparées à la ligne de base (800 ms) au moyen de l'ANOVA et du test de t de Student. ***Résultats :*** L'ECG a déclenché la SMT des voies du NCXI avec une fiabilité de 100%. Les amplitudes des PEM ont été diminuées à proximité de l'OPA, particulièrement à 120 ms (0,21 ± 0,04 mV versus 0,39 ± 0,10 mV ; p = 0,003). Les probabilités de décharge du trapèze étaient inhibées de façon similaire (43,8% versus 88.2% ; p = 0,009). Aucun effet de proximité de l'OPA n'a été observé du côté non atteint (p = 0,868). L'examen a été bien toléré. ***Conclusions :*** Une compression vasculaire peut causer la mononeuropathie du NCXI. Le couplage SMT-cardiovasculaire est une technique qui permet d'évaluer les interactions à la jonction neuro-vasculaire et de diagnostiquer une CNV de façon non effractive.

Can. J. Neurol. Sci. 2009; 36: 83-88

Vascular compression probably underlies many cranial mononeuropathies[1] but is controversial[2,3] and lacks a definitive diagnostic investigation. Imaging may identify cerebrovascular abnormalities associated with cranial mononeuropathies.[4,5] However, diagnosis of potential neurovascular compression (NVC) syndromes such as trigeminal neuralgia or hemifacial spasm is usually clinical, lacking proof of the underlying mechanism. Resulting uncertainty creates difficulty in decision making for microvascular decompression surgery and limits studies of pathophysiology.

Only a single case of progressive CNXI palsy with evidence of vascular compression has been reported.[6] The intimate anatomical relationship between the posterior inferior cerebellar artery (PICA) and CNXI[7] combined with cases of regional vascular diseases associated with CNXI palsy[8-11] or overactivity[12,13] support vascular etiologies for CNXI mononeuropathy.

From the Division of Neurology, Alberta Children's Hospital (AK), University of Calgary, Calgary, Alberta; Division of Neurology, Toronto Western Research Institute (CG, RC), University of Toronto, Toronto, Ontario, Canada.

Received May 14, 2008. Final Revisions Submitted July 23, 2008.

Correspondence to: Adam Kirton, Division of Neurology, Department of Pediatrics, Alberta Children's Hospital, 2888 Shaganappi Trail NW, Calgary, Alberta, T6B 3A8, Canada.

Transcranial magnetic stimulation (TMS) provides safe, non-invasive stimulation of corticobulbar pathways.[14] Transcranial magnetic stimulation studies have defined the normal electrophysiological properties of pathways between the motor cortex and the CNXI-innervated muscles: sternocleidomastoid (SCM) and trapezieus (TPZ).[14,15] We report a case of CNXI palsy secondary to vascular compression and describe a novel method coupling cardiovascular physiology with TMS to provide evidence of NVC.

Methods

Clinical Case

A patient diagnosed with chronic, progressive CNXI mononeuropathy secondary to vascular compression was recruited. The patient was followed for 20 years and all previous medical records and investigations were reviewed. Informed consent for participation and image publication was obtained.

Hypothesis

We hypothesized that the repeated impact of the arterial pressure wave (APW) on CNXI at the neurovascular junction responsible for the mononeuropathy would transiently alter TMS-induced motor evoked potentials (MEP) transmitted through CNXI to TPZ. This effect would manifest as an inhibition of MEP transmission with resulting decreases in both amplitude and probability of MEP firing that would be time-locked to the APW and cardiac cycle.

Arterial Pressure Wave (APW) and Transit Time (APWTT)

The APW is generated with left ventricular contraction and distributed through the arterial tree at a rate dependent on multiple variables including arterial size and stiffness.[16] The patient was a healthy 34-year-old at the time of study with no vascular disease risk factors. Distance between the left ventricular apex and PICA origin from vertebral artery (VA) along the arterial tree (aorta → left subclavian → left vertebral → left PICA) was calculated from body measurements and MRI. Age-dependent APW values[16] were then used to calculate possible values for the time required for the APW to travel to the PICA origin. This APW transit time (APWTT) had a range of 43-85 msec.

Central motor conduction time (CMCT) is that required for a TMS-induced cortical impulse to exit the central nervous system[17] and ranges from 5-6ms for CNXI-innervated muscles.[14] Using these APWTT and CMCT values, a range of times during which the effect of the APW on TMS-induced TPZ MEP's was determined (Table). Hypothesizing an interaction of brief but unknown duration, intervals were tested from the earliest possible interaction (40ms) to beyond the APWTT range for late or delayed effects. Employing increments of 40ms generated stimulation intervals of 40, 80, 120, and 160ms. Based on patient heart rate (HR), a time-point 90% removed from the previous QRS was taken as baseline to minimize the possibility of APW effect.

Neuro-cardiovascular coupling to TMS

Two surface electrocardiographic (ECG) electrodes were placed over the precordium. Locations were adjusted to produce a pronounced, rapid deflection of the QRS from baseline to facilitate computer software triggering. The patient sat in a large, comfortable chair with the head in a neutral position with SCM and TPZ relaxed. Based on previous publications[15] and preliminary studies with the patient, recordings from the SCM were less reliably obtained and, therefore, only TPZ recordings were employed. Surface EMG electrodes were placed over the center of the upper third of TPZ muscle bellies bilaterally.

Using a figure-of-eight coil (Magstim Company, Dyfed, UK) at slightly suprathreshold stimulation intensities (50% maximum stimulator output), the motor hotspots for both TPZ muscles were determined. Beginning over parasaggital motor strip[15] and moving in 5 mm increments, the location producing the largest MEP was determined and marked on the scalp. Rest motor threshold was determined bilaterally (intensity required to obtain MEP >50μV in 5/10 trials). Active motor threshold (AMT, intensity to obtain >100μV in 5/10 trials) was determined bilaterally during voluntary activation of TPZ to 30% of maximum (visual and auditory feedback using an oscilloscope).

The experimental set-up is diagrammed in Figure 1A. Both ECG and MEP potentials were input to a desktop computer and displayed on screen (Signal software 3.07, Cambridge Electronic Design, Cambridge, UK). Signals were amplified, filtered (2Hz to 2.5kHz), digitized at 5kHz (Micro 1401, Cambridge Electronics Design, Cambridge, UK) and stored for offline analysis. Suprathreshold stimuli of 120% AMT were applied for all measurements with the TPZ activated to 30% of maximum. The initial QRS deflection on ECG was used for software triggering of TMS at time intervals of 40, 80, 120, 160 and 800ms (control). Ten stimulation trials at each interval were delivered in random order six seconds apart. This series was repeated on the affected side for a total of 100 stimuli and once on the unaffected side (50 stimuli).

Peak-to-peak MEP amplitude for each trial was measured offline. A software script was applied to raw tracing data to extract measurable deflections from baseline background activity, including both spontaneous and TMS-induced MEP. All tracings were reviewed by the same blinded investigator. Only MEP originating from stable baseline were accepted while those

Table: Pulse Transit Time (PTT)

	Distance	APW Velocity	APWTT
Minimum time	39.0 cm	Stiff, smallest size 900 cm/sec	43.3 ms
Maximum time	42.2 cm	Healthy, largest 500 cm/sec	84.4 ms

The range of possible APW transit times (APWTT) to reach the left PICA origin from the left ventricle was calculated using the patient's anatomical imaging and established APW reference values. APWTT = APW velocity / distance.

https://doi.org/10.1017/S0317167100006363 Published online by Cambridge University Press

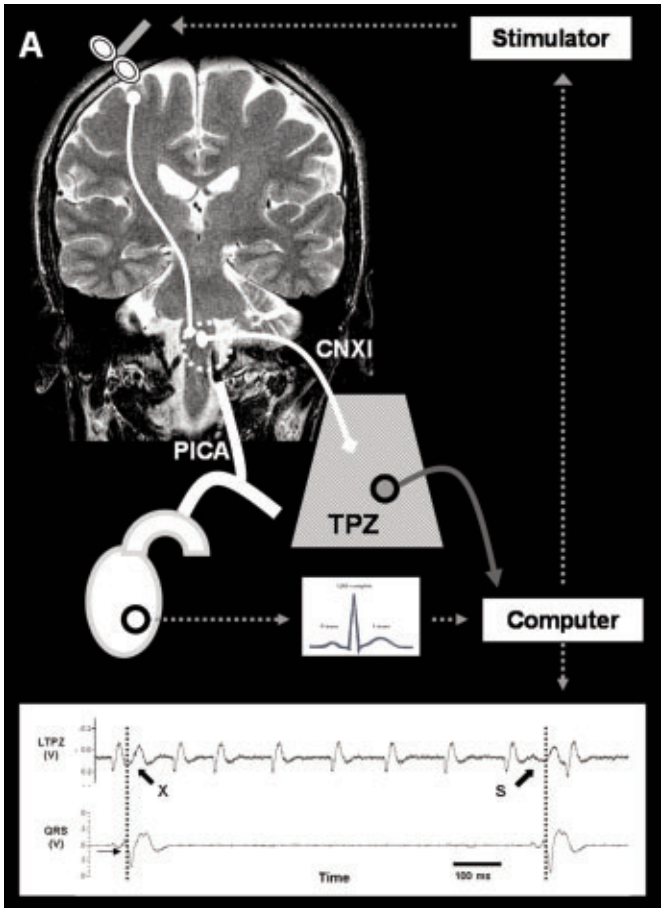

Figure 1: *Experimental set-up. (A) Initiation of the APW at the left ventricle was captured with ECG (QRS) and transmitted to the computer. The APW travels along the arterial tree to interact with CNXI at the PICA origin. At set time intervals from the QRS, the computer triggered the central stimulation (TMS coil) of the spinal accessory pathway. The transmitted stimulus was recorded as an MEP over the contralateral TPZ. Only MEP triggered from a steady baseline (S) were analyzed while those coinciding with spontaneous potentials (X) were excluded. (Bottom Panel) Stimulations were delivered at intervals from the QRS within and beyond the range of calculated PTT (40-160ms, A-D). Baseline recordings were obtained at point E (880ms).*

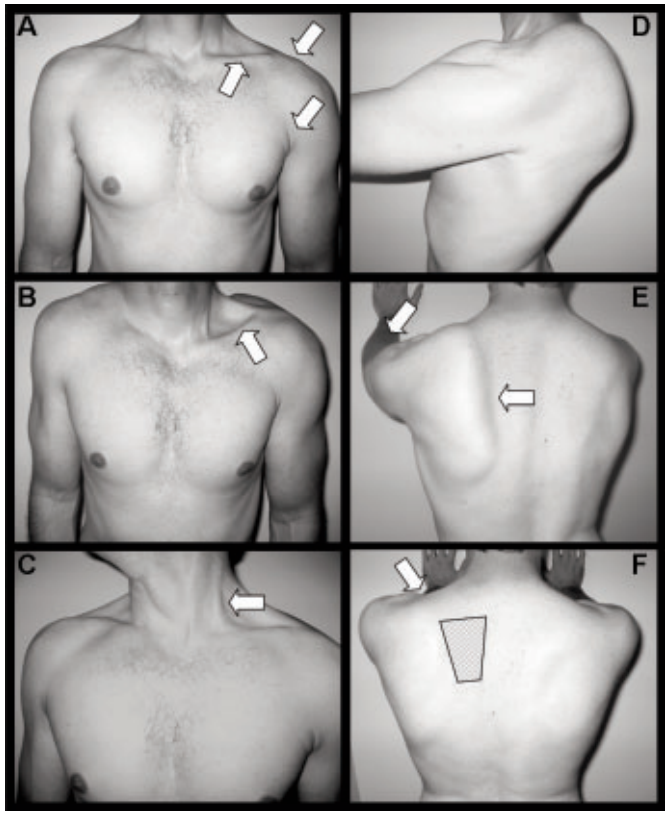

Figure 2: *Spinal accessory mononeuropathy. Patient demonstrates marked atrophy of the left TPZ with depression of the left shoulder and axillary skin folds (A). Shoulder shrugging exaggerates the atrophy with supraclavicular hollowing (B). Right head turn demonstrates left SCM atrophy (C). Shoulder flexion produces scapular winging (D), exaggerated with pushing with elbow flexed (E), but less evident with elbow fully extended (F). The area of notalgia paresthetica is outlined (F).*

in proximity to spontaneous EMG potentials were excluded (Figure 1A, bottom). Since the reduced number of motor-units on the affected side resulted in essentially "all-or-none" MEP generation, a firing probability rate (number potentials >0.10 mV / total number of stimulations) was calculated for each time interval.

Statistical Analysis

One-way ANOVA was applied across all intervals to detect differences in mean MEP amplitudes. Each of the states coupled to the APW were compared to the baseline state (800ms) using the student t-test following testing to assure both normalcy of the data (method of Kolmogorov and Smirnov) and equal SD between groups (method of Bartlett). Bonferroni post-hoc analysis was employed as a conservative means of correction for the effect of multiple comparisons. Nonparametric firing rate data was analyzed using Chi-square and Fisher exact tests to detect differences between baseline and APW-coupled states. Statistical analyses were performed using SAS software (version 9.1.3).

Results

Case Report

A 34 year-old right-handed male had first noticed extra left axillary skin folds at the age of 16 years. His family physician noted decreased left paraspinal muscle bulk but no action was taken. Nine years later, progressive, involuntary "twitching" of the left SCM and TPZ was reported. Within six months, significant wasting of both muscles was evident. The patient noted difficulty abducting the left arm above 90 degrees but had

https://doi.org/10.1017/S0317167100006363 Published online by Cambridge University Press

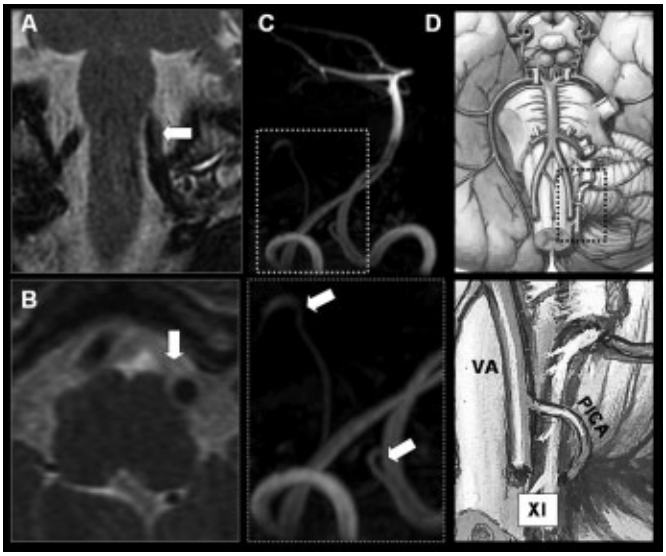

Figure 3: *Neurovascular compression imaging. Coronal (A) and axial (B) T2 MRI demonstrate VA compression of the ventrolateral medulla. (C, inset) MRA demonstrates a large, tortuous PICA (top arrow) including an acute angle between the VA and PICA origin (bottom arrow). (D, inset) CNXI passes through this narrow space where it is subject to neurovascular compression (reprinted with permission[29]).*

no other complaints. He was otherwise healthy and review of systems, past medical history, and family history were unremarkable.

On examination, marked weakness and wasting of the left SCM and TPZ (Figure 2A-C) with frequent fasciculations was observed. The left shoulder was depressed and the patient had difficulty abducting beyond 90 degrees, requiring supination of the arm and recruitment of additional muscles. There was marked scapular winging with shoulder flexion that was pronounced with pushing (reduced with elbow extension, Figure 2D-F). Retrospective review of personal photographs demonstrated gradual progression of the shoulder deformity and muscle wasting over more than 10 years.

Nerve conduction and electromyography confirmed chronic dennervation mononeuropathy of the left CNXI and was otherwise normal including bilateral testing of serratus anterior (long thoracic nerve) and multiple muscles of the upper and lower limbs. Initial brain MRI at 26 years was interpreted as normal. Additional MRI studies were completed at 29 and 32 years including MR angiography (MRA) and high-resolution studies of the brainstem, skull base, and cervical spine including gadolinium enhancement and fat saturation sequences. Retrospective review of all imaging demonstrated stable compression of the anterolateral left medulla by the left VA (Figure 3A, B). MRA demonstrated an unusually large left PICA with a hyperacute angle between its origin and the VA(Figure 3C) through which CNXI was thought to pass (Figure 3D).[7] No significant clinical change occurred between the three MR studies and alternative diagnoses including intraxial, extra-axial, or jugular foramen neoplasms were excluded.

At 31 years, the patient began experiencing a sensory disturbance over the left paraspinal region. He described a tingling, "pins and needles" sensation over a trapezoid-shaped area of approximately 12 cm diameter in the left paraspinal region from T1-T6 (Figure 2F). Symptoms would occur spontaneously 1-3 times per day without precipitation, lasting 1-5 minutes. Examination demonstrated normal appearing skin with decreased sensation to both light touch and pinprick and intact temperature sensation. By 32 years, the patient began experiencing moderate episodes of pruritis in the same area several times per day. A diagnosis of notalgia paresthetica secondary to scapular winging was made.

Now at 34 years, the patient has remained stable with complete atrophy of the left SCM and TPZ. He suffers no shoulder pain or significant physical limitations and his driving distance in golf has improved with progression of the scapular winging, perhaps related to the resulting increased freedom of rotation of the left upper extremity around the torso. The working diagnosis is chronic progressive spinal accessory mononeuropathy secondary to vascular compression.

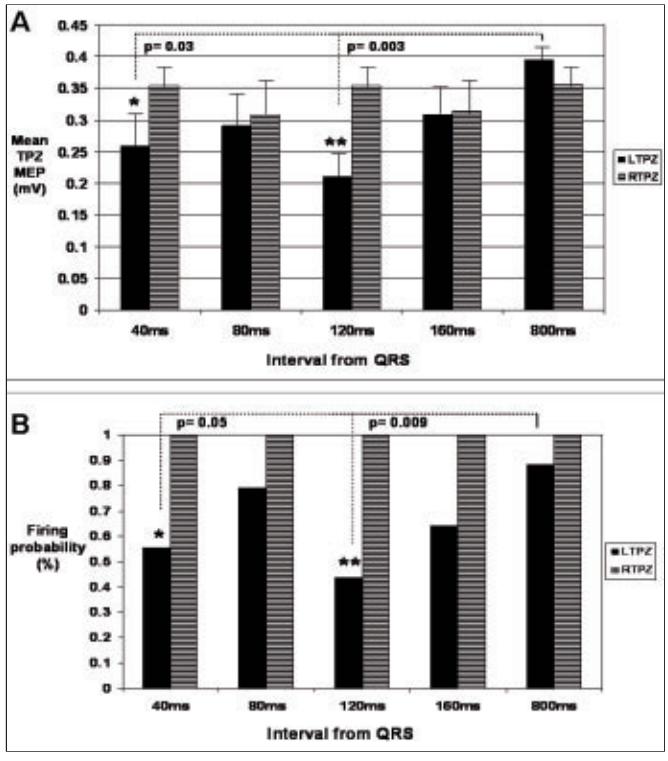

Figure 4: *Effect of APW on TPZ MEP amplitude and firing probability. (A) Mean amplitude of left TPZ MEP (black bars) is significantly decreased from baseline (800ms) at 120 ms, approximating the interaction of the APW at the neurovascular junction between PICA and CNXI. No difference is seen on the unlesioned right side (hatched bars). (B) Firing probability demonstrates a similar effect at 120 ms (black bars) with 100% firing at all intervals on the unaffected side (hatched bars). Values are mean mV and % respectively ± SEM.*

https://doi.org/10.1017/S0317167100006363 Published online by Cambridge University Press

TMS neurophysiology of CNXI

The atrophic left TPZ demonstrated no spontaneous surface EMG activity at rest. Right motor cortex stimulation at 100% of stimulator output did not produce any TPZ rest MEP. With activation to 30% of maximum, a markedly reduced interference pattern with regular EMG discharges was obtained (Figure 1). Most were of similar morphology, suggesting activation of a single motor unit, though multiple units could be recruited with effort. The AMT for the left TPZ was 73% of stimulator output.

The non-lesioned (right) TPZ demonstrated properties consistent with previously published norms.[14,15] Active motor threshold of the right TPZ was 62% of stimulator output. The motor hotspot for both sides was similar, located approximately 0.5cm lateral to the vertex over the inter-aural line. No adverse events were experienced during TMS though the patient reported a marked increase in frequency of left TPZ and SCM fasciculations that lasted two to three weeks.

TMS neuro-cardiovascular coupling

Transcranial magnetic stimulation was triggered by ECG with 100% reliability. Blinded analysis of neurophysiological data resulted in the exclusion of only 14% of trials where MEP coincided with spontaneous discharges. The proportion of rejected trials did not differ between the 5 intervals (range 11-16%).

On the affected side, the baseline state at 800ms showed mean MEP amplitude of 0.39±0.10 mV. Motor evoked potentials amplitude was dramatically reduced at 120ms (0.21±0.04 mV, p=0.003) and satisfied the Bonferroni correction for multiple comparisons (adjusted p-value <0.0125). Lesser effects were observed at the 40ms interval (0.26±0.05 mV, p=0.03) as well as 80ms (0.29±0.07 mV, p=0.08) and 160ms (0.31±0.09 mV, p=0.14). One-way analysis of variance (ANOVA) across all states suggested a greater variation among state means than expected by chance though this did not reach statistical significance (p=0.09). No differences were seen between the different time intervals on the unaffected right side including ANOVA (p=0.8676) and t-tests (all p>0.35). Tests for both normalcy and consistency of standard deviation were satisfied. The MEP amplitude results are summarized in Figure 4A.

A similar effect of proximity to the APW was observed for firing rate probability on the affected side. Probability of left TPZ firing was markedly reduced from baseline (800 ms) at the 120ms interval (43.8% versus 88.2%, p=0.009). Similar to MEP amplitude, insignificant trends were also seen at the 40ms interval (52.9% versus 88.2%, p=0.05) while no differences were found at 80ms (61.3%, p=0.21) or 160ms (71.4%, p=0.64). The unaffected right side demonstrated 100% firing across all states. Firing probability results are summarized in Figure 4B.

Discussion

We present a novel method coupling cardiovascular physiology to stimulation of CNXI pathways with TMS to suggest their pathological interaction at the neurovascular junction. While results are preliminary, this technique could provide a non-invasive means of confirming NVC in cranial mononeuropathy.

The direct apposition and subsequent pathological interaction of PICA and CNXI are supported by detailed studies of PICA anatomy.[7] Our patient's vertebral-PICA anatomy followed a common pattern, including origin of PICA from the lateral medullary segment with a large PICA loop. Within this arrangement, the most common course of PICA includes either direct passage through XI rootlets or the space between CNX and CNXI, consistent with the model, neuroimaging, and neurophysiological data presented here.

Significant limitations are acknowledged including the single case nature of the study. A severe degree of muscle wasting complicated assessment of MEP's where a limited number of motor units produced "all-or-none" firing rather than the range of MEP obtained from more intact muscle. How the long-standing injury to the spinal accessory nerve itself influenced our assessments is also unknown. However, that our measurement of both amplitude and firing rate showed the same significant, time-locked effect of the APW illustrates consistency. Finally, the rarity of previous CNXI NVC reports raises the question of diagnostic accuracy. However, the diagnosis is strongly supported by the slow progression of the palsy, vascular abnormalities on neuroimaging, and the exclusion of alternative diagnoses over 20 years of investigation. To overcome these limitations, this method now needs to be applied to a larger cohort of patients with more common NVC syndromes such as hemifacial spasm or trigeminal neuralgia. Studying individuals both pre and post MVD surgery would be particularly valuable.

Maximum effect of the APW on both MEP amplitude and firing rate were observed at the same time interval of 120ms. While this consistency suggests the effect may be real, the time falls just beyond our estimated APWTT range of 40-80ms (Table). The effect of the APW on cranial nerve function is not well understood and likely complex. That the 40ms time interval may also be decreased supports our original hypothesis of a "direct", early, and inhibitory effect of the APW on CNXI transmission. That firing probability was similarly decreased raises consideration of a conduction block mechanism though evidence supporting this is difficult to glean from a single study of a patient with such pronounced dennervation. That the APW effects appeared maximal at 120ms may suggest additional, more complex inhibitory effects on nerve function after the APW has passed. More data is required to address these hypotheses.

Also suggesting complexity to NVC effects on cranial nerve function is the variety of conditions reported that include both pathological over-activity and palsy. In addition to trigeminal neuralgia and hemifacial spasm, other examples of NVC-induced pathological increases in activity include glosso-pharyngeal neuralgia (IX), tinnitus/vertigo (VIII) and superior oblique myokymia (IV)[3,18,19] as well as spasmodic torticollis with CNXI compression.[12,13] However, loss of function and palsy predominate in other NVC cranial neuropathies including occulomotor (III),[20] trochlear (IV), abducens (VI),[21,22] acoustic (VIII),[23] and hypoglossal (XII)[24] lesions. It is possible that the negative symptoms of some unilateral NVC CN palsies, especially when onset is gradual, could be under-recognized due to minimal symptomology (e.g. glossopharyngeal palsy).

CNXI compression is unusual in that both palsy[6,10,11] and overactivity[12,13] have been reported. Facial or trigeminal motor atrophy is not described in the common syndromes involving CNV and VII, suggesting differences in pathophysiology. Ephaptic transmission has been postulated as an underlying mechanism in hyperactive syndromes such as trigeminal

https://doi.org/10.1017/S0317167100006363 Published online by Cambridge University Press

neuralgia,[25] suggesting an interaction between sensory and motor components of cranial nerves. In contrast, pure motor nerves may be more likely to show only palsy, such as our case and others including cranial nerves III,[20] VI,[21,22] and XII.[24] In contrast, compression of sensory cranial nerves may feature hyperactivity without palsy (V, VII, IX). That most of these syndromes consist of small numbers of cases must be considered, as well as those nerves where both patterns have been demonstrated (e.g VIII). A detailed analysis of a large number of NVC cases is beyond the scope of this paper but could provide a means to test this hypothesis.

Notalgia paresthetica (NP) is a rare and poorly understood dermatologic condition characterized by a hypoesthetic patch over the medial scapular border, often accompanied by intense itching or burning and dyspigmentation. Increasing evidence suggests disorders of the spine, particularly those leading to impingement of dorsal spinal nerves, may be responsible.[26] Notalgia paresthetica was reported in a young patient with transient long thoracic nerve palsy secondary to neuralgic amyotrophy where marked scapular winging was suggested to cause dysfunction of dorsal spinal nerves.[27] Notalgia paresthetica associated with CNXI lesions has not been reported to our knowledge but we would suggest the same mechanism was responsible in our case.

The safe, non-invasive, and relatively simple nature of TMS creates a valuable neurophysiological investigational tool. A case-control TMS study demonstrated changes in contralateral post-excitatory cortical inhibition in patients with hemifacial spasm and suggested its utility in distinguishing organic from functional cases.[28] While this method does not address the NVC issue at the level of the primary problem (neurovascular junction) as we have attempted, it suggests that combined approaches with TMS may be particularly useful in the diagnostic evaluation of NVC syndromes.

References

1. Wilkins RH. Neurovascular compression syndromes. Neurol Clin. 1985;3:359-72.
2. Adams CB. Microvascular compression: an alternative view and hypothesis. J Neurosurg. 1989;70:1-12.
3. Monstad P. Microvascular decompression as a treatment for cranial nerve hyperactive dysfunction--a critical view. Acta Neurol Scand Suppl. 2007;187:30-3.
4. Kuncz A, Voros E, Barzo P, Tajti J, Milassin P, Mucsi Z et al. Comparison of clinical symptoms and magnetic resonance angiographic (MRA) results in patients with trigeminal neuralgia and persistent idiopathic facial pain. Medium-term outcome after microvascular decompression of cases with positive MRA findings. Cephalalgia. 2006;26:266-76.
5. Holley P, Bonafe A, Brunet E, Simonetta-Moreau M, Manelfe C. [The contribution of "time-of-flight" MRI-angiography in the study of neurovascular interactions (hemifacial spasm and trigeminal neuralgia)]. J Neuroradiol. 1996;23:149-56.
6. Lunardi P, Mastronardi L, Farah JO, De BC, Trasimeni G, Gualdi GF. Spinal accessory nerve palsy due to neurovascular compression. Report of a case diagnosed by magnetic resonance imaging and magnetic resonance angiography. Neurosurg Rev. 1996;19:75-8.
7. Macchi V, Porzionato A, Parenti A, De CR. The course of the posterior inferior cerebellar artery may be related to its level of origin. Surg Radiol Anat. 2004;26:60-5.
8. Vincentelli F, Caruso G, Rabehanta PB, Rey M. Surgical treatment of a rare congenital anomaly of the vertebral artery: case report and review of the literature. Neurosurgery. 1991;28:416-20.
9. Kitagawa M, Nakagawa Y, Kitaoka K, Kobayashi N, Ishikawa T, Nagashima M. [Accessory nerve paralysis due to compression of the fenestrated vertebral artery]. No Shinkei Geka. 1988;16: 1173-7.
10. Magoni M, Scipione V, Anzola GP. Isolated accessory nerve palsy of unusual cause. Ital J Neurol Sci. 1994;15:241-3.
11. Kikuchi K, Kowada M, Kojima H. Hypoplasia of the internal carotid artery associated with spasmodic torticollis: the possible role of altered vertebrobasilar haemodynamics. Neuroradiology. 1995;37:362-4.
12. Pagni CA, Naddeo M, Faccani G. Spasmodic torticollis due to neurovascular compression of the 11th nerve. Case report. J Neurosurg. 1985;63:789-91.
13. Shima F, Fukui M, Matsubara T, Kitamura K. Spasmodic torticollis caused by vascular compression of the spinal accessory root. Surg Neurol. 1986;26:431-4.
14. Berardelli A, Priori A, Inghilleri M, Cruccu G, Mercuri B, Manfredi M. Corticobulbar and corticospinal projections to neck muscle motoneurons in man. A functional study with magnetic and electric transcranial brain stimulation. Exp Brain Res. 1991;87:402-6.
15. Pelliccioni G, Scarpino O, Guidi M. Magnetic stimulation of the spinal accessory nerve: normative data and clinical utility in an isolated stretch-induced palsy. J Neurol Sci. 1995;132:84-8.
16. O'Rourke MF, Staessen JA, Vlachopoulos C, Duprez D, Plante GE. Clinical applications of arterial stiffness; definitions and reference values. Am J Hypertens. 2002;15:426-44.
17. Hess CW. Central motor conduction and its clinical application. In: Magnetic stimulation in clinical neurophysiology. Hallet M, Chokroverty S, editors. Co 2005, Elsevier, Inc, Philadelphia, PA; page 86.
18. Hashimoto M, Ohtsuka K, Suzuki Y, Minamida Y, Houkin K. Superior oblique myokymia caused by vascular compression. J Neuroophthalmol. 2004;24:237-9.
19. Yousry I, Dieterich M, Naidich TP, Schmid UD, Yousry TA. Superior oblique myokymia: magnetic resonance imaging support for the neurovascular compression hypothesis. Ann Neurol. 2002;51: 361-8.
20. Hashimoto M, Ohtsuka K, Akiba H, Harada K. Vascular compression of the oculomotor nerve disclosed by thin-slice magnetic resonance imaging. Am J Ophthalmol. 1998;125: 881-2.
21. Ohtsuka K, Sone A, Igarashi Y, Akiba H, Sakata M. Vascular compressive abducens nerve palsy disclosed by magnetic resonance imaging. Am J Ophthalmol. 1996;122:416-9.
22. Zhu Y, Thulborn K, Curnyn K, Goodwin J. Sixth cranial nerve palsy caused by compression from a dolichoectatic vertebral artery. J Neuroophthalmol. 2005;25:134-5.
23. Wahlig JB, Kaufmann AM, Balzer J, Lovely TJ, Jannetta PJ. Intraoperative loss of auditory function relieved by microvascular decompression of the cochlear nerve. Can J Neurol Sci. 1999;26:44-7.
24. Morini A, Rozza L, Manera V, Buganza M, Tranquillini E, Orrico D. Isolated hypoglossal nerve palsy due to an anomalous vertebral artery course: report of two cases. Ital J Neurol Sci. 1998;19:379-82.
25. Hilton DA, Love S, Gradidge T, Coakham HB. Pathological findings associated with trigeminal neuralgia caused by vascular compression. Neurosurgery. 1994;35:299-303.
26. Savk O, Savk E. Investigation of spinal pathology in notalgia paresthetica. J Am Acad Dermatol. 2005;52.1085-7.
27. Tacconi P, Manca D, Tamburini G, Cannas A, Giagheddu M. Notalgia paresthetica following neuralgic amyotrophy: a case report. Neurol Sci. 2004;25:27-9.
28. Kotterba S, Tegenthoff M, Malin JP. Hemifacial spasm or somatoform disorder--postexcitatory inhibition after transcranial magnetic cortical stimulation as a diagnostic tool. Acta Neurol Scand. 2000;101:305-10.
29. Netter FH. Cerebral vasculature. In: Atlas of human anatomy. Netter FH, Colacino S, editors. Co 1989 CIBA-GEIGY Corporation, West Caldwell NJ. plate 132.